Radiotherapy and Oncology 102 (2012) 309–314

Contents lists available at SciVerse ScienceDirect

Radiotherapy and Oncology

journal homepage: www.thegreenjournal.com

Esophageal cancer

Residual setup errors and dose variations with less-than-daily image guided patient setup in external beam radiotherapy for esophageal cancer ☆

Chunhui Han [a,*], Daniel C. Schiffner [b], Timothy E. Schultheiss [a], Yi-Jen Chen [a], An Liu [a], Jeffrey Y.C. Wong [a]

[a] Department of Radiation Oncology, City of Hope National Medical Center, Duarte, CA, USA; [b] Department of Radiation Oncology, University of California, Irvine, CA, USA

ARTICLE INFO

Article history:
Received 31 January 2011
Received in revised form 14 June 2011
Accepted 13 July 2011
Available online 27 August 2011

Keywords:
Esophageal cancer
Setup error
Megavoltage CT
Image guidance

ABSTRACT

Background and purpose: To evaluate residual patient setup errors and daily dose variations of different less-than-daily image guidance (IG) strategies in the delivery of external beam radiotherapy for esophageal cancer.

Material and methods: Daily image-guided setup data for 25 consecutive esophageal cancer patients treated with helical tomotherapy were evaluated. Seven less-than-daily IG strategies with different imaging frequencies were simulated. For each IG strategy, the daily residual setup errors were calculated. Using TomoTherapy Planned Adaptive software, daily dose variations to the clinical target volume, heart, and lungs were evaluated in five representative patients.

Results: With 0% (60%) IG frequency, the margins required for adequate coverage of the clinical target volume were 13 mm (10 mm), 14 mm (11 mm), and 5 mm (5 mm) in the left–right, superior–inferior, and anterior–posterior directions, respectively. Even with 60% IG frequency, 10% of the fractions had more than 10% decrease in the dose level covering 95% of the target, and 14% and 13% of the fractions had more than 10% increase in total lung volume receiving at least 0.8 Gy per fraction, and heart volume receiving at least 1.2 Gy per fraction, respectively.

Conclusion: Substantial residual setup errors would occur for treatment fractions without IG even if the most frequent less-than-daily IG strategy was to be used, which could lead to significant daily dose variations for the target volume and adjacent normal tissues. Daily image guidance is recommended throughout the course of treatment in conformal radiotherapy for esophageal cancer.

 Radiotherapy and Oncology 102 (2012) 309–314

Radiotherapy plays an important role in multimodality management of esophageal cancer [1,2]. Due to the proximity of the target volume to critical organs including the lungs and the heart, external beam radiotherapy treatment for esophageal cancer is especially challenging for treatment planning and patient setup [3]. Intensity modulated radiotherapy (IMRT), which provides a highly conformal dose distribution through the modulation of beam fluence, can be used to achieve significant sparing of critical organs [4,5]. Due to a sharp dose gradient outside the target volumes with IMRT plans, accurate target alignment and patient positioning are crucial to ensure adequate dosimetric coverage of the target volumes and avoidance of the adjacent normal structures.

Recent studies found that significant setup variations could occur during radiotherapy treatment of esophageal cancer, if only skin mark alignment is used during patient setup [6,7]. Daily image-guided setup techniques, such as those using three-dimensional mega- or kilo-voltage imaging, portal imaging, and ultrasound imaging, can be used to reduce patient setup errors. However, daily image guidance (IG) is associated with added costs in terms of additional time with the treatment machine, additional work and training required for the therapy staff, patient imaging dose, and capital expenses associated with acquiring and maintaining the needed technologies. These added costs need to be justified for the adoption of daily IG.

Instead of employing IG on a daily basis for patient alignment, less frequent IG strategies have been used [8,9]. Studies have been performed on the residual setup errors associated with different IG strategies in the delivery of external beam radiotherapy to treat prostate and head-and-neck cancers, respectively [10,11]. These investigations found that increasing IG frequency led to smaller residual systematic patient setup errors while residual random setup errors were not significantly affected.

To date, no prior study has investigated whether reasonable positioning accuracy can be achieved by using any less-than-daily IG strategies in the treatment of this disease site. Therefore this study was carried out to evaluate residual patient positioning

☆ This study was presented during the 2008 Annual Meeting of the American Society of Radiation Oncology (ASTRO).

* Corresponding author. Address: Department of Radiation Oncology, City of Hope National Medical Center, Duarte, CA 91010, USA.

E-mail address: chan@coh.org (C. Han).

0167-8140/$ - see front matter
doi:10.1016/j.radonc.2011.07.027

errors and the resulting daily dosimetric variations for different less-than-daily IG strategies in the treatment of esophageal cancer.

Materials and methods

Twenty-five consecutive esophageal cancer patients who underwent neoadjuvant chemoradiation therapy using helical tomotherapy (TomoTherapy Hi-Art System, TomoTherapy Inc., Madison, Wisconsin) between 2004 and 2008 were included in this study. Table 1 lists patient characteristics. All the patients had mid- or distal esophageal cancer. Details about treatment planning and image registration procedures were described previously [6]. Briefly, prior to treatment planning, each patient received a kilovoltage computed tomography (kVCT) scan using a big-bore CT simulator (AcQSim CT, Philips Healthcare, Eindhoven, The Netherlands). During the CT scan, as well as during daily treatments, the patients were instructed to maintain shallow breathing to minimize internal organ motion due to respiration. The spiral kVCT scans were performed with 3 mm axial slice thickness and spacing using a pitch of 1.7. The axial CT image resolution was 512×512 pixels with a field of view of 48–60 cm. Patients were scanned head first in the supine position with their arms placed above the head by using a wingboard (Med-Tec, Orange City, Iowa). A custom Vac-Loc device (Med-Tec, Orange City, Iowa) was used to immobilize the lower extremities of the patient. Three tattoos were placed on the upper torso (midline at the level of the xiphoid as well as at the right and left mid-axillary lines) to serve as reference points for daily patient alignment with the in-room laser coordinate system.

The planning CT studies were transferred to a treatment planning system (Eclipse 8.0, Varian Medical Systems Inc., Palo Alto, California) for contouring of critical organs and target volumes. The gross target volume (GTV) was defined as the primary tumor plus involved lymph nodes by imaging studies including CT scan, positron-emission tomography (PET) scan, and endoscopic ultrasound. The clinical target volume (CTV) was defined as the GTV with a 5-cm margin in the superior and inferior directions and a 2-cm margin laterally, based on historical conformal therapy experience [12–14], to account for microscopic tumor expansions and internal organ motion of the tumor. Since daily image-guided setup corrections were used prior to each treatment fraction, a uniform 4-mm margin was applied to the CTV to form the planning target volumes (PTV). The images and structure set were transferred to the helical tomotherapy planning station through the DICOM-RT protocol. The axial image resolution was downgraded to 256×256 pixels in the helical tomotherapy system. A uniform total dose 45 Gy in 25 fractions was prescribed for the PTV.

Prior to each treatment fraction, patients were immobilized on the treatment table using the same immobilization devices as during the planning CT scan. Therapists then positioned the patient by aligning the patient skin marks in the in-room laser coordinate system. An MVCT scan was performed in the thoracic region, encompassing the entire PTV with a minimum longitudinal dimension of three-vertebral-body lengths. The MVCT scans were performed with a pitch of three and a slice thickness of 6 mm. Each axial slice had a field of view of 40 cm in diameter. The MVCT images were automatically registered with the planning kVCT images based on bony anatomy using a mutual information algorithm [15,16]. The image registration utilized three rigid translations in the left–right (LR), superior–inferior (SI), and anterior–posterior (AP) directions, as well as roll (rotation around the SI axis). After the automatic image registration, the radiation therapists also performed manual rigid image registrations to ensure proper alignment of soft tissue in the CTV region under the supervision of the attending radiation oncologist. Occasionally, significant mismatch existed between the superior and the inferior parts of the target volume due to rotational error. The patient was then re-positioned and a new MVCT scan was performed. The translational setup corrections were applied by shifting the treatment couch, and the roll corrections were applied by adjusting the beam-on angle of the gantry.

Table 1
Patient characteristics.

Number of Patients	25
Male/Female	19/6
Age (year), mean (range)	65.7 (30–87)
Height (cm), mean (range)	172 (147–193)
Weight (kg), mean (range)	85.2 (50.3–123.7)
Body mass index (kg·m^{-2}), mean (range)	28.9 (18.5–42.3)
GTV volume (cm^3), mean ± SD (range)	118.2 ± 68.0 (30.7–279.9)
GTV Length (cm), mean ± SD (range)	7.8 ± 2.3 (3.6–11.4)
Total Number of MVCT scans	625 (25 patients × 25 fractions)

SD, standard deviation.

Seven less-than-daily IG scenarios, together with the actual daily IG, were evaluated:

1. Scenario A (0% IG): In this scenario, the patient would simply be set up on the treatment couch based on alignment of the skin tattoos in the laser coordinate system. Since the helical tomotherapy treatment couch sags slightly as it moves into the gantry, a systematic error existed in the AP direction. In addition, the initial lateral position of the treatment couch had an intrinsic offset from the initial position of the planning CT couch, leading to a systematic error in the lateral position. The average shifts in all the fractions were applied to each fraction to eliminate these systematic errors.
2. Scenarios B (12% IG) and C (20% IG) were similar to the de Boer no-action-level (NAL) strategy [8], where IG is performed on the first three and five fractions, respectively. The average couch shifts in each axis for the initial three (Scenario B) or five (Scenario C) fractions were then applied to all the subsequent fractions.
3. Scenario D (20% IG) involved IG once a week. The shift made at the beginning of each week would be applied to the subsequent four fractions, if a >3 mm difference was found in any direction compared with the shifts in the previous week.
4. Scenario E (36% IG) was similar to the de Boer extended no-action-level (eNAL) strategy [9]. IG was performed in the first five fractions and once per week thereafter. The running mean shift was applied to subsequent non-IG fractions.
5. Scenario F (52%) utilized IG every other day, using the running mean of setup corrections to correct subsequent non-IG fractions.
6. Scenario G (60% IG) used IG on the first five fractions, followed by IG every other day. The running mean was applied to subsequent non-IG fractions.

In external beam radiotherapy, the overall setup errors consist of a systematic component and a random component. We adopted the van Herk methodology [17] for analysis of patient positioning errors. The average of individual systematic setup errors in the cohort is denoted by μ, the standard deviation (SD) of individual systematic setup errors is denoted by Σ, and the average of individual random errors is denoted by σ. In the analysis of residual setup errors, μ, Σ, and σ were calculated for treatment fractions without IG. A CTV-to-PTV margin of $2.5\Sigma + 0.7\sigma$ was used as the optimal margin to ensure that $\geqslant$95% of the prescribed dose is delivered to $\geqslant$99% of the CTV [17,18].

Daily dose variations with less-than-daily IG strategies, as well as the actual daily IG strategy, were evaluated using the Planned

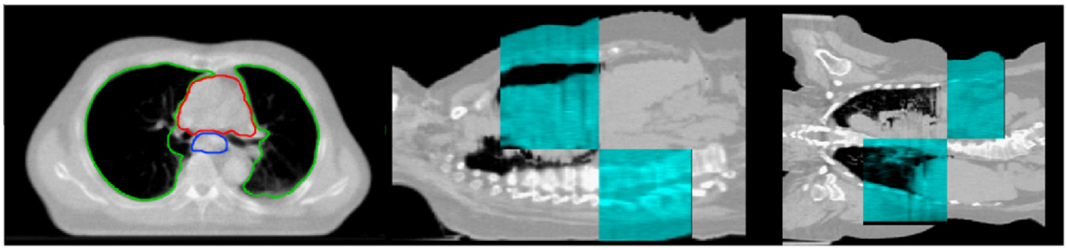

Fig. 1. Representative axial, sagittal, and coronal MVCT images. Contours were drawn on the axial image. Blue: GTV; red: heart; green: total lung.

Adaptive (Version 3.1, TomoTherapy Inc., Madison, Wisconsin) software application [19]. Due to the labor intensity of contouring and dose calculation with each IG scenario, daily dose variations under five IG scenarios (Scenarios A, C, E, G, and actual daily IG) were calculated for five randomly selected patients. The average GTV volume for these five patients was 140.1 ± 102.5 cm^3, with average length of 8.9 ± 2.2 cm in the SI direction.

For each of the five patients, contours of the GTV, lungs, and heart were drawn on each daily MVCT image set by the physician. The GTV contour on the registered planning CT images was used as guidance for contouring the GTV on the MVCT images. Fig. 1 shows a representative axial MVCT image with contours. The same GTV-to-CTV margins used during treatment planning were applied to the GTV in the MVCT images to form the CTV. To calculate the daily dose distribution, the MVCT images were first registered and fused to the planning CT images by applying the setup corrections under each IG scenario. The dose fluence map from the treatment plan was applied to the combined CT images, and the daily dose distribution under each scenario was calculated [20]. Since each MVCT scan encompassed the entire PTV and the regions of the heart and lungs receiving high dose, this technique enabled us to analyze the actual doses delivered to the CTV, heart, and lungs and generate dose-volume histogram data for these structures. For each treatment fraction, the following dosimetric parameters were analyzed:

1. CTV D95: the dose level that covers 95% of the CTV in the analyzed fraction.
2. Heart V1.2: the heart volume receiving ⩾1.2 Gy in the analyzed fraction.
3. Lung V0.8: the total lung volume receiving ⩾0.8 Gy in the analyzed fraction.

1.2 Gy per fraction to the heart and 0.8 Gy per fraction to the lungs correspond to 30 and 20 Gy over the 25-fraction course of treatment, respectively. Since the MVCT scan did not always encompass the complete heart and lungs, the absolute volumes of heart V1.2 and lung V0.8 were used. These values, among other dosimetric parameters, are clinically-relevant dosimetric parameters related to the risk of morbidity to the heart and the lungs, respectively [21–23].

Table 3
The optimal CTV-to-PTV expansion margins in each IG scenario required to ensure that ⩾95% of the prescribed dose is delivered to ⩾99% of the CTV, based on the van Herk formula ($2.5\Sigma + 0.7\sigma$).

Scenario	IG frequency (%)	CTV-to-PTV margin/mm		
		LR	SI	AP
A	0	13	14	5
B	12	13	14	7
C	20	12	14	6
D	20	10	9	7
E	36	12	10	6
F	52	11	11	7
G	60	10	11	5

Results

Table 2 lists statistics of residual patient setup errors with each IG scenario. With increasing IG frequency from 0% to 60%, no significant variations in average random errors (σ) were observed in any direction. However, the SD of systematic setup errors (Σ) showed a trend of reduction in the SI and LR directions with increasing IG frequency. For actual daily patient setup corrections for treatments delivered to the 25 patients, the average overall setup corrections (μ) were 1.5 mm in the LR direction, −1.9 mm in the SI direction, and 0.8 mm in the AP direction. The average overall setup corrections were used to eliminate the systematic setup error component in Scenario A. The average and SD of roll corrections were −0.35 ± 1.63°.

The optimal CTV-to-PTV margins for each IG scenario are listed in Table 3. We found a slight reduction for margins in the LR and SI directions with increasing IG frequency. However, even with an IG frequency of 60%, rather large CTV-to-PTV margins of 10, 11, and 5 mm were still required in the LR, SI, and AP axis, respectively.

Fig. 2 evaluates the magnitude and frequency of occurrence of residual setup errors in all the treatment fractions with each IG scenario. With IG frequency increasing from 0% to 60%, the percentage of treatment fractions with >6 mm setup errors decreased from 31.0% to 11.0% in the LR direction, from 32.3% to 9.1% in the SI direction, from 5.0% to 1.3% in the AP direction, and from 65.0% to 20.5% for the 3D vector of displacement. There was no significant

Table 2
Systematic and random patient setup errors in non-IG fractions in each less-than-daily IG scenario. All the units are in millimeters (mm).

Scenario	IG frequency (%)	LR			SI			AP		
		μ	Σ	σ	μ	Σ	σ	μ	Σ	σ
A	0	1.5	3.5	5.7	−1.9	4.3	4.6	0.8	1.2	3.0
B	12	−0.6	3.6	5.6	−1.5	4.4	4.4	−1.7	2.2	2.4
C	20	−0.5	3.1	5.8	−1.6	4.2	4.3	−0.5	1.8	2.4
D	20	0.1	2.2	7.1	−0.5	2.2	5.7	−1.3	1.6	4.7
E	36	−0.1	3.3	5.7	−1.5	2.8	4.4	−0.2	1.5	2.5
F	52	0.0	2.6	5.9	−1.2	3.2	4.2	−2.2	1.8	3.3
G	60	−0.3	2.6	5.7	−1.3	3.3	3.9	−0.8	1.4	2.0

μ, mean systematic error; Σ, SD of systematic error; σ, average random error.

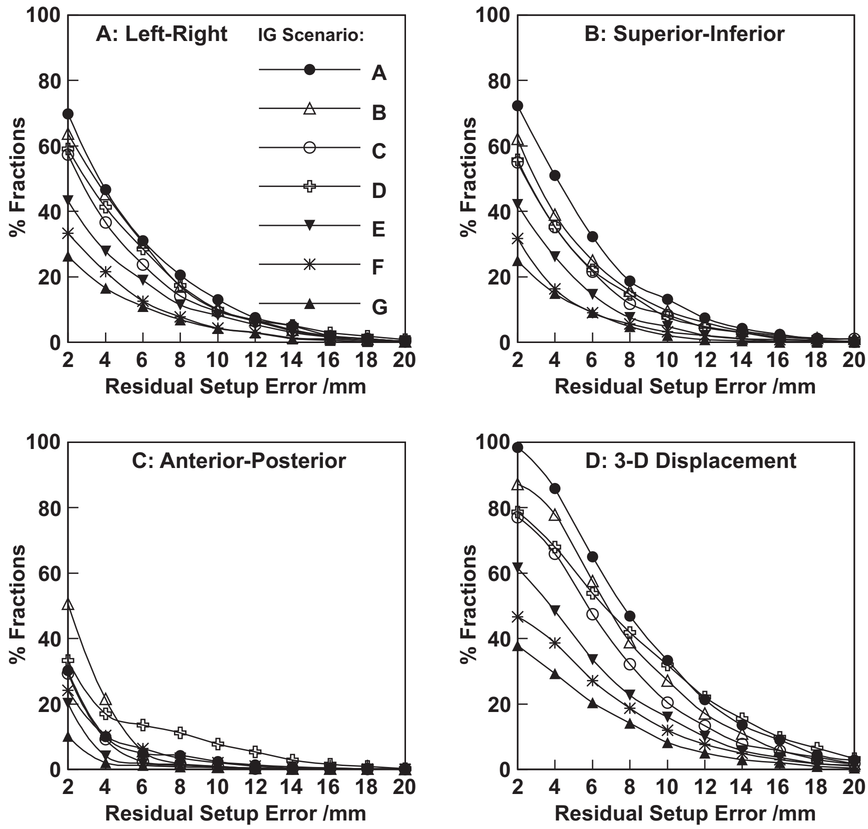

Fig. 2. Magnitude and frequency of occurrence of residual setup errors under each IG scenario in the LR direction (A), SI direction (B), AP direction (C), and three-dimensional vector of displacement (D), where the 3D vector of displacement is calculated as the square root of the quadratic sum of setup errors along each axis.

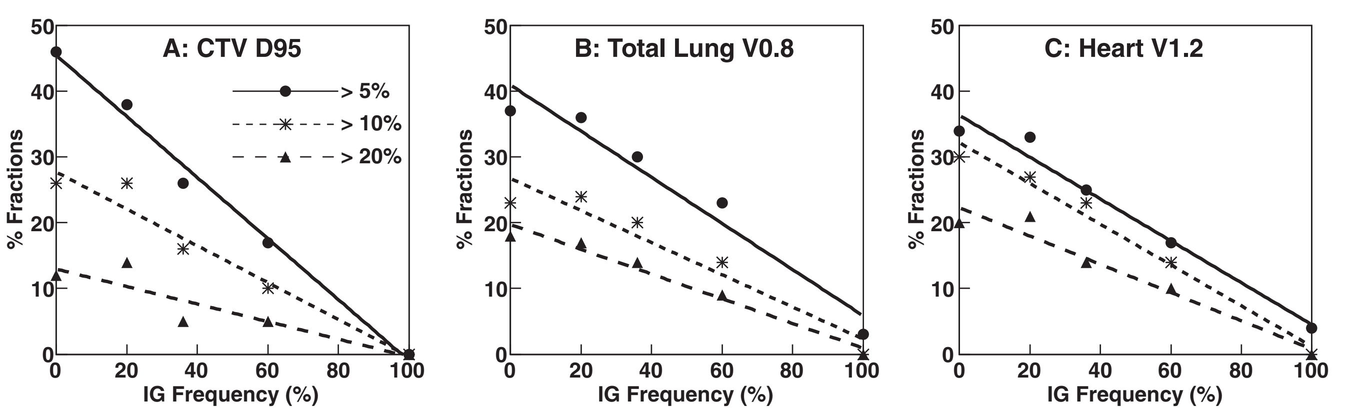

Fig. 3. Percentage of fractions with decrease in CTV D95 (A), increase in total lung V0.8 (B), and increase in heart V1.2 (C) by 5%, 10%, and 20%, respectively, with IG scenarios A (0% IG frequency), C (20%), E (36%), G (60%), and daily IG (100%).

trend of variation with IG frequency in the AP direction, likely due to the small number of fractions with large setup errors.

For the five patients selected for dosimetric analysis, the overall standard deviations of daily shifts were 5.1, 7.0, and 3.0 mm in the LR, SI, and AP directions, respectively. In comparison, the overall standard deviations of daily shifts were 6.6, 6.2, and 3.1 mm in the LR, SI, and AP directions, respectively, for all the 25 patients. Fig. 3 evaluates the percentage of treatment fractions with decrease in CTV D95 (A), increase in total lung V0.8 (B), and increase in heart V1.2 (C) by 5%, 10%, and 20%, respectively, under each of the five IG scenarios. With increasing IG frequency from 0% to 100%, the percentage of fractions with significant underdosing of the CTV and overdosing of the total lung and heart decreased in a linear fashion. With the use of daily IG, we found no >10% decrease of CTV D95 or >10% increase of total lung V0.8 or heart V1.2 in any treatment fraction. However, even with 60% IG frequency, >10% decrease in CTV D95 was observed in 10% of the fractions, and >10% increase in total lung V0.8 and heart V1.2 were observed in 14% and 13% of the fractions, respectively.

Discussion

Implementation of daily IG in external beam radiotherapy to treat esophageal cancer is associated with added costs discussed in the Introduction. These costs must be weighed against the potential improvement in accuracy of daily patient alignment. In the current study, we evaluated the residual setup errors resulting from each of seven less-than-daily IG scenarios and the optimal CTV-to-PTV margins that would be required for the fractions without IG. In addition, we measured the dosimetric consequences to the CTV, heart, and total lung resulting from these errors in patient alignment. In short, we found that even with the most frequent IG scenario, significant residual patient setup errors still occurred in a substantial number of fractions, which lead to underdosing of the CTV and delivery of excessive doses to the heart and total lung.

In principle, the systematic component of setup errors can be estimated and reduced by analyzing a sample of daily setup errors. By analyzing daily setup errors for a significant portion of fractions, a good estimate of the systematic setup errors can be calculated and used to correct systematic errors in the remaining treatment fractions. In the current study, with IG frequency increasing from 0% to 60%, the standard deviations of systematic setup errors (Σ) were reduced by 26% and 23% in the LR and SI directions, respectively. On the other hand, daily random setup errors cannot be eliminated by applying uniform corrections. More reproducible patient immobilization techniques and the introduction of pretreatment IG-based patient setup are strategies that can be utilized to reduce random setup errors. Even with these strategies, proper margins must be maintained to account for intra-fractional organ motion as well as uncertainty in the IG process.

Compared to the setup error analysis for prostate cancer patients with different IG strategies performed by Kupelian et al. [10], our study showed that increasing IG frequency had a smaller effect on the residual setup errors for non-IG treatment fractions. Indeed, by increasing imaging frequency from 0% to 60%, the required margins for non-IG treatment fractions only changed from 13 to 10 mm in the LR direction, from 14 to 11 mm in the SI direction, and showed no substantial change in the AP direction.

This finding is likely due to differences in the treatment site and immobilization techniques between the two studies. In our study, random patient setup errors were a more significant component of overall patient setup errors. As a consequence, significant residual setup errors remained even with 60% IG frequency, as more than 50% of the non-IG fractions had >6 mm residual patient setup errors in terms of the 3D vector of displacement. Instead of the 4-mm uniform CTV-to-PTV margin employed in our treatment plans, margins of 10, 11, and 5 mm in the LR, SI, and AP directions, respectively, would be needed to ensure adequate CTV dosimetric coverage in the non-IG treatment fractions with Scenario G, which could lead to increased toxicity to adjacent normal organs.

Note that in this study, the 4-mm CTV-to-PTV margin only accounted for setup uncertainty, while the GTV-to-CTV margin accounted for both microscopic tumor extension and intra-fractional internal organ motion. The magnitude of the GTV-to-CTV margin was based on historical experiences with conformal radiotherapy [12–14]. In modern radiotherapy, the internal organ motion was represented by a separate margin to the CTV to form the internal target volume (ITV) [24]. With modern imaging technologies, internal esophageal motion has been studied in recent years. Using daily CT images, Cohen et al. suggested asymmetric margins of 8–12 mm in the axial plane for internal organ motion [25]. Dieleman analyzed internal organ motion for normal esophagus using four-dimensional CT [26], and suggested 9 mm lateral and 8 mm dorsal–ventral margins for distal esophagus, and 7 mm lateral and 6 mm dorsal–ventral margins for mid-esophagus. On the other hand, Hawkin et al. evaluated overall setup errors for esophageal cancer patients using cone-beam CT [7], and suggested margins of 5, 7, and 5 mm in the LR, SI, and AP directions, respectively.

Despite having only 20% IG frequency, Scenario D showed relatively smaller standard deviation of systematic errors in the LR and SI directions (Table 2), indicating smaller CTV-to-PTV margins in the LR and SI directions (Table 3). The daily shifts data showed that there were systematic variations of daily shifts in the later phase of the treatment course for some patients. Compared to other IG strategies (except Scenario A) which generally relied on shifts in IG fractions at the beginning of the treatment, Scenario D used shifts data from the most recent IG fraction to make setup corrections for non-IG fractions. Therefore, the setup correction strategy in Scenario D could adapt to systematic changes more quickly.

With the widespread implementation of three-dimensional conformal radiotherapy (3D-CRT) and IMRT, accurate patient positioning has become a more critical issue due to rapid dose fall-off outside of the PTV. Geometric misses could readily occur during IMRT treatment if tight margins are used without accurate patient positioning. Indeed, even with Scenario G, the dosimetric coverage of the CTV, in terms of CTV D95, was reduced by >5% in 17% of fractions and by >10% in 10% of fractions. Furthermore, the total lung V0.8 and heart V1.2 were increased by >10% above the planned values in 14% and 13% of fractions, respectively, with Scenario G. Such dose deviations could compromise clinical outcomes in terms of decreased tumor control and increased normal organ toxicity. We found that large dosimetric errors were prevented in all fractions that employed pretreatment IG-based patient alignment.

Although MVCT images generally have lower image quality compared to kVCT images, previous studies have shown that MVCT images still provides reasonable image contrast for delineating many soft tissue structures [27,28]. In this study, GTV contouring in MVCT images was aided by the presence of surrounding high-contract organs, including the lungs laterally and the vertebral column posteriorly. However, the 6-mm axial slice thickness in the MVCT images led to intrinsic uncertainty in both image registration and GTV contours.

With daily MVCT based setup corrections, some concerns exist about the extra dose associated with the imaging scans. Shah et al. evaluated patient dose from helical tomotherapy MVCT scans [29]. With a pitch of 2, the mean dose to the normal organs in the thoracic region was <1.5 cGy, and the maximum dose was <2.0 cGy in most cases. When a pitch of three is used in MVCT scans, the imaging dose is scaled by a factor of 0.67. With a prescription dose of 2 Gy per fraction, the extra dose to the normal tissue contributed by daily MVCT is small (<1% of the prescription dose). Given the benefits of daily IG in terms of positional and dosimetric error reduction that was shown in this study, we feel that the use of daily MVCT-based patient alignment is both justified and advisable in the treatment of esophageal cancer with conformal radiotherapy.

Conclusion

Even with 60% IG frequency, significant residual setup errors still occurred in external beam radiotherapy to treat esophageal cancer, which resulted in significant dose deviations from the treatment plan in terms of compromised coverage of the CTV and the delivery of excessive dose to the adjacent heart and lungs. With any less-than-daily IG strategy, rather large CTV-to-PTV margins are needed, which could lead to increased normal organ toxicity. Daily IG is recommended for the optimal treatment of esophageal cancer with conformal radiation therapy techniques.

Conflict of interest

None declared.

References

[1] Berger B, Belka C. Evidence-based radiation oncology: oesophagus. Radiother Oncol 2009;92:276–90.

[2] Geh JI, Bond SJ, Bentzen S, Glynne-Jones R. Systematic overview of preoperative (neoadjuvant) chemoradiotherapy trials in oesophageal cancer: evidence of a radiation and chemotherapy dose response. Radiother Oncol 2006;78:236–44.
[3] Asakura H, Hashimoto T, Zenda S, et al. Analysis of dose-volume histogram parameters for radiation pneumonitis after definitive concurrent chemoradiotherapy for esophageal cancer. Radiother Oncol 2010;95:240–4.
[4] Chandra A, Guerrero TM, Liu HH, et al. Feasibility of using intensity-modulated radiotherapy to improve lung sparing in treatment planning for distal esophageal cancer. Radiother Oncol 2005;77:247–53.
[5] Chen YJ, Liu A, Han C, et al. Helical tomotherapy for radiotherapy in esophageal cancer: a preferred plan with better conformal target coverage and more homogeneous dose distribution. Med Dos 2007;32:166–71.
[6] Chen YJ, Han C, Liu A, et al. Setup variations in radiotherapy of esophageal cancer: evaluation by daily megavoltage computed tomography localization. Int J Radiat Oncol Biol Phys 2007;68:1537–45.
[7] Hawkins MA, Aitken A, Hansen VN, McNair HA, Tait DM. Set-up errors in radiotherapy for oesophageal cancers – Is electronic portal imaging or conebeam more accurate? Radiother Oncol 2011;98:249–54.
[8] de Boer HC, van Os MJ, Jansen PP, et al. Application of the no action level (NAL) protocol to correct for prostate motion based on electronic portal imaging of implanted markers. Int J Radiat Oncol Biol Phys 2005;61:969–83.
[9] de Boer HC. Heijmen, BJM, and eNAL: an extension of the NAL setup correction protocol for effective use of weekly follow-up measurements. Int J Radiat Oncol Biol Phys 2007;67:1586–95.
[10] Kupelian PK, Lee C, Langen KM, et al. Evaluation of image-guidance strategies in the treatment of localized prostate cancer. Int J Radiat Oncol Biol Phys 2008;70:1151–7.
[11] Zeidan OA, Langen KM, Meeks SL, et al. Evaluation of image-guidance protocols in the treatment of head and neck cancers. Int J Radiat Oncol Biol Phys 2007;67:670–7.
[12] Minsky BD, Pajak TF, Ginsberg RJ, et al. INT 0123 (Radiation Therapy Oncology Group 94–05) phase III trial of combined-modality therapy for esophageal cancer: high-dose versus standard-dose radiation therapy. J Clin Oncol 2002;20:1167–74.
[13] Tepper J, Krasna MJ, Niedzwiecki D, et al. Phase III trial of trimodality therapy with cisplatin, fluorouracil, radiotherapy, and surgery compared with surgery alone for esophageal cancer: CALGB 9781. J Clin Oncol 2008;26:1086–92.
[14] Walsh TN, Noonan N, Hollywood D, et al. A comparison of multimodal therapy and surgery for esophageal adenocarcinoma. N Engl J Med 1996;335:462–7.
[15] Ruchala KJ, Olivera GH, Kapatoes JM. Limited-data image registration for radiotherapy positioning and verification. Int J Radiat Oncol Biol Phys 2002;54:592–605.
[16] Boswell S, Tome W, Jeraj R, et al. Automatic registration of megavoltage to kilovoltage CT images in helical tomotherapy: an evaluation of the setup verification process for the special case of a rigid head phantom. Med Phys 2006;33:4395–404.
[17] van Herk M, Remeijer P, Rasch C, et al. The probability of correct target dosage: dose-population histograms for deriving treatment margins in radiotherapy. Int J Radiat Oncol Biol Phys 2000;47:1121–35.
[18] van Herk M. Errors and margins in radiotherapy. Semin Radiat Oncol 2004;14:52–64.
[19] Langen KM, Meeks SL, Poole DO, et al. The use of megavoltage CT (MVCT) images for dose recomputation. Phys Med Biol 2005;50:4259–76.
[20] Han C, Chen YJ, Liu A, et al. Actual dose variation of parotid glands and spinal cord for nasopharyngeal cancer patients during radiotherapy. Int J Radiat Oncol Biol Phys 2008;70:1256–62.
[21] Gagliardi G, Constine LS, Moiseenko V, et al. Radiation dose-volume effects in the heart. Int J Radiat Oncol Biol Phys 2010;76:S77–85.
[22] Marks LB, Bentzen SM, Deasy JO, et al. Radiation dose-volume effects in the lung. Int J Radiat Oncol Biol Phys 2010;76:S70–6.
[23] Wei X, Liu HH, Tucker SL, et al. Risk factors for pericardial effusion in inoperable esophageal cancer patients treated with definitive chemoradiation therapy. Int J Radiat Oncol Biol Phys 2008;70:707–14.
[24] Lorchel F, Dumas JL, Noël A, Wolf D, Bosset JF, Aletti P. Esophageal cancer: determination of internal target volume for conformal radiotherapy. Radiother Oncol 2006;80:327–32.
[25] Cohen RJ, Paskalev K, Litwin S, et al. Esophageal motion during radiotherapy: quantification and margin implications. Dis Esophagus 2010;23:473–9.
[26] Dieleman EMT, Senan S, Vincent A, et al. Four-dimensional computed tomographic analysis of esophageal mobility during normal respiration. Int J Radiat Oncol Biol Phys 2007;67:775–80.
[27] Meeks SL, Harmon JF, Langen KM, et al. Performance characterization of megavoltage computed tomography imaging on a helical tomotherapy unit. Med Phys 2005;32:2673–81.
[28] Forrest LJ, Mackie TR, Ruchala K, et al. The utility of megavoltage computed tomography images from a helical tomotherapy system for setup verification purposes. Int J Radiat Oncol Biol Phys 2004;60:1639–44.
[29] Shah AP, Langen KM, Ruchala KM, et al. Patient dose from megavoltage computed tomography imaging. Int J Radiat Oncol Biol Phys 2008;70:1579–87.